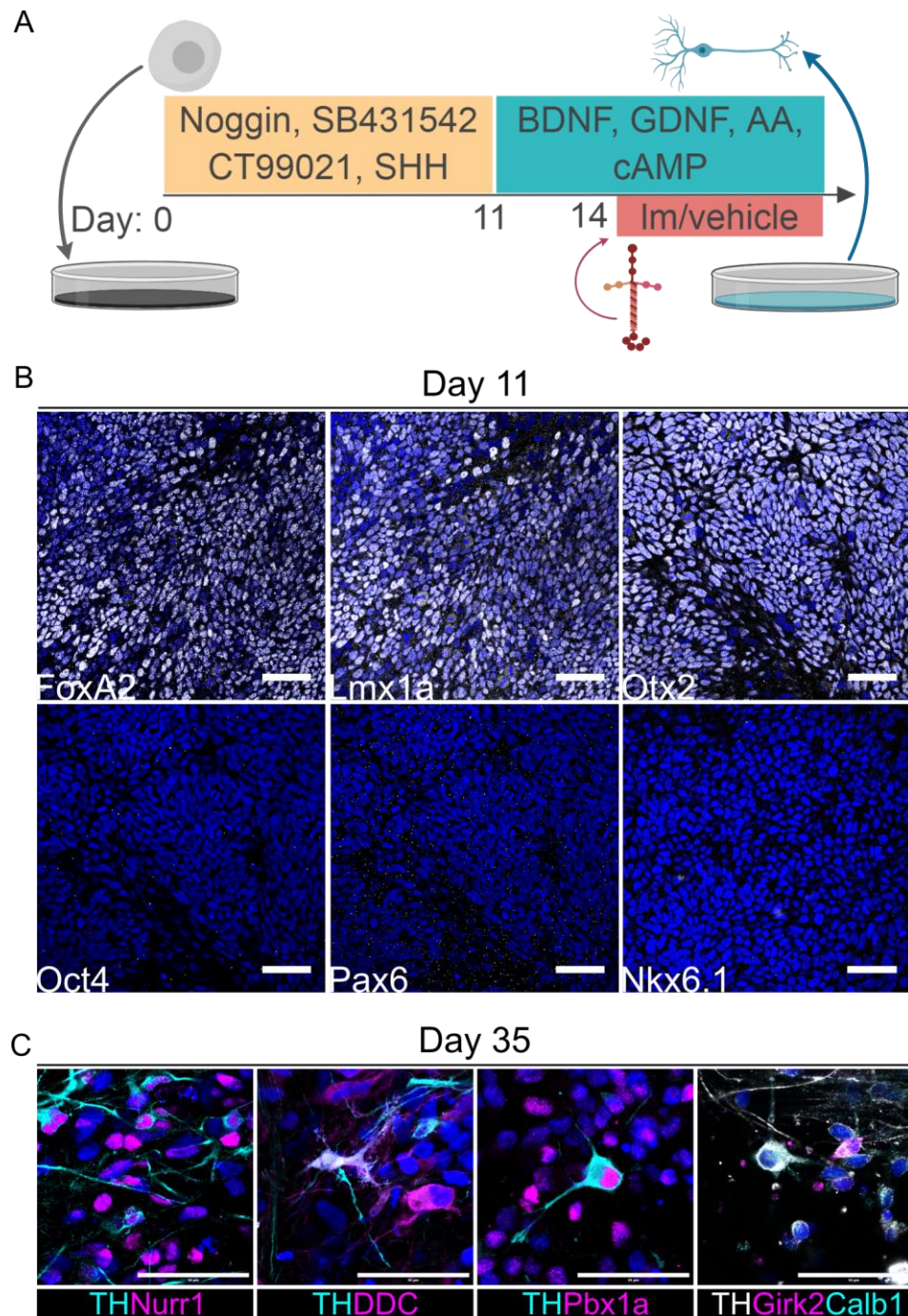
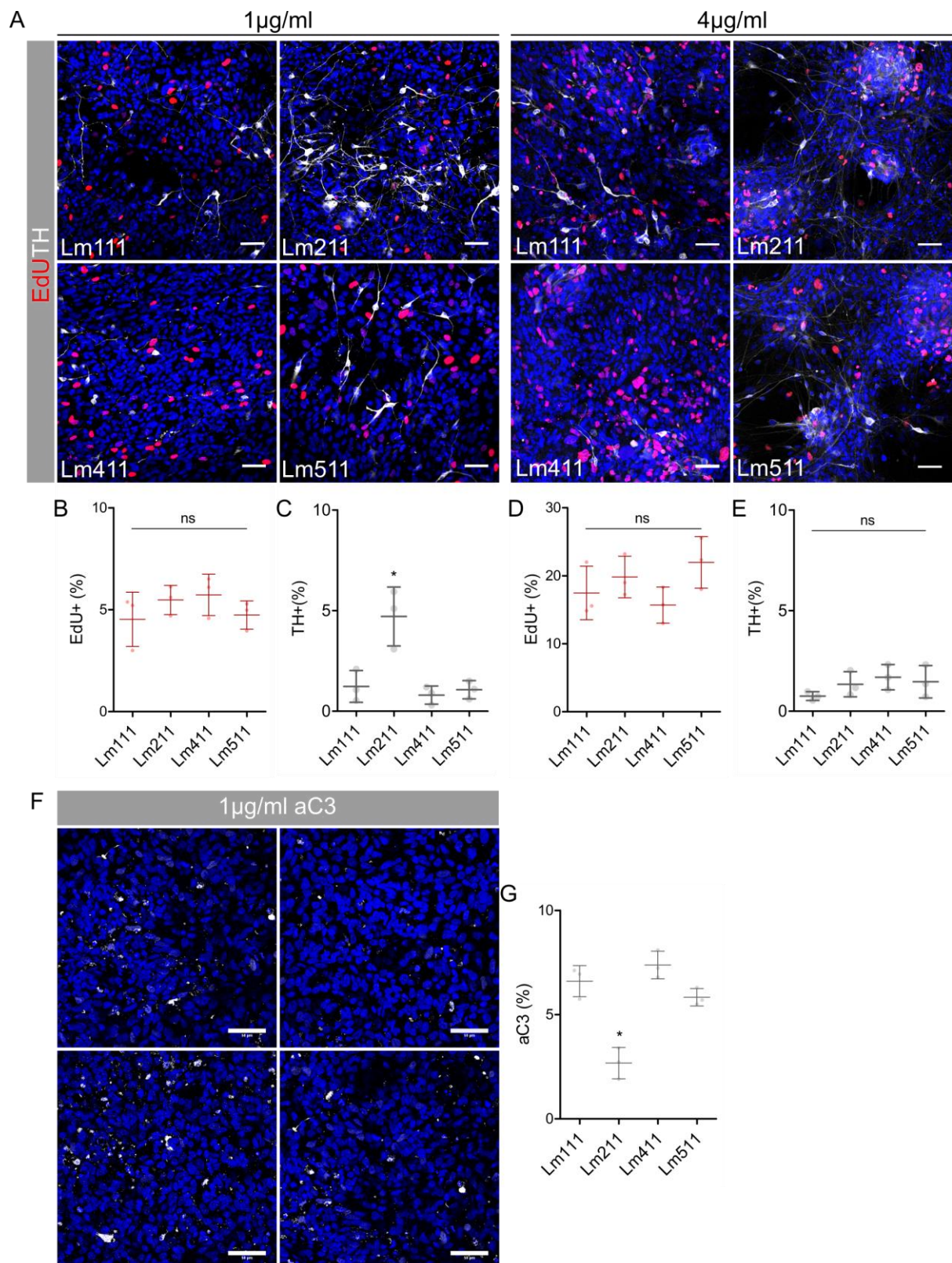


Fig S1: Lm- α chain immunohistochemistry in human VM

(A) Lm- α 1 expression is restricted to the basement membrane surrounding the basal surface neural tube. Lm- α 3 is not expressed in the human VM. Lm- α 4 is restricted to the basal laminae of blood vessels at both 6 and 10 pcw. Meanwhile Lm- α 5 is expressed on both the ventricular and basal surfaces of the VM at 6 pcw as well as some interstitial expression. (B) scRNA-seq data of individual Lm- α chains showing cell types for gene expression in human development. Right axis shows absolute molecule counts. (C) Lm- α 2 expression in the mouse VM at E10.5-E14.5 displays a similar expression pattern as that seen in the human embryo. Expression can be seen to diminish over time with negligible positive expression at E14.5.

**Fig S2: Differentiation protocol and patterning of hES cells into mDA progenitors**

(A) schematic of hES differentiation protocol with Im treatment at day 14 till fixation. (B) Immunostainings of day 11 cultures showing cultures to be triple positive for the mDA progenitor markers FoxA2, Lmx1a and Otx2. Cultures are negative for the pluripotency marker Oct4, forebrain marker Pax6 and the lateral domain marker Nkx6.1. (C) TH+ Neurons at day 35 showing positive immunoreactivity for a panel of markers (Nurr1, Pbx1a, DDC, Calb1, Girk2) illustrative of bona fide mDA neurons. Scale bar 50 μ m.

**Fig S3: Lm isoform specificity in regulating mDA progenitor proliferation and survival**

(A) Representative images of mDA cultures at day 28 exposed to Lm211 at 1 and 4 $\mu\text{g ml}^{-1}$, staining for proliferation (EdU) and neurons (TH). At low concentrations (1 $\mu\text{g ml}^{-1}$), no significant difference in proliferation (B) is detected between any of the Lm isoforms whilst an increase in TH+ mDA neurons (C) is observed on Lm211. At high concentrations (4 $\mu\text{g ml}^{-1}$), no differences are detected in the number of mDA progenitors that are EdU+ (D) or TH+ (E). (F,G) Significantly fewer aC3+ cells can be seen at 1 $\mu\text{g ml}^{-1}$ of Lm211 suggesting the increase in TH+ neurons is due to increased survival.

* $p < 0.001$, ANOVA Tukey's post test, N=3

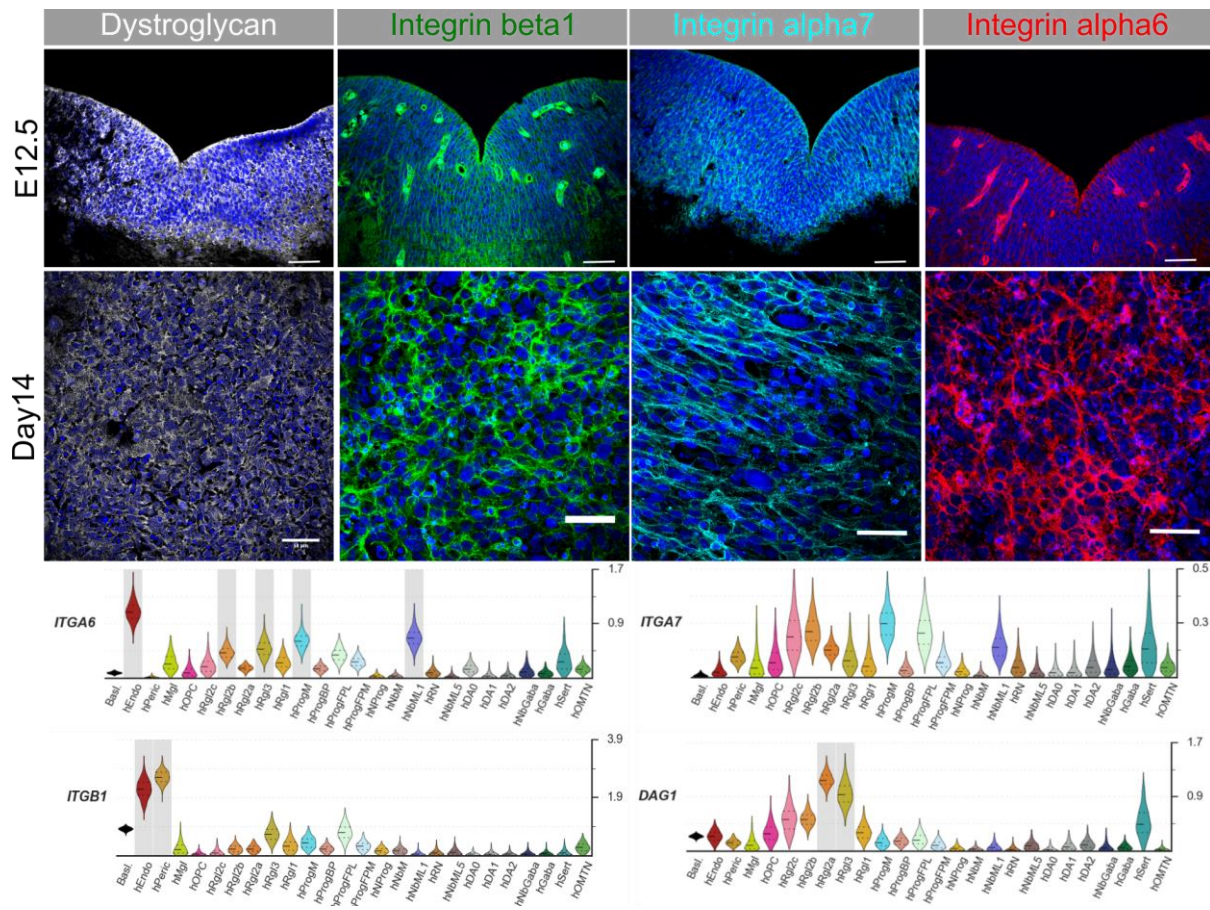
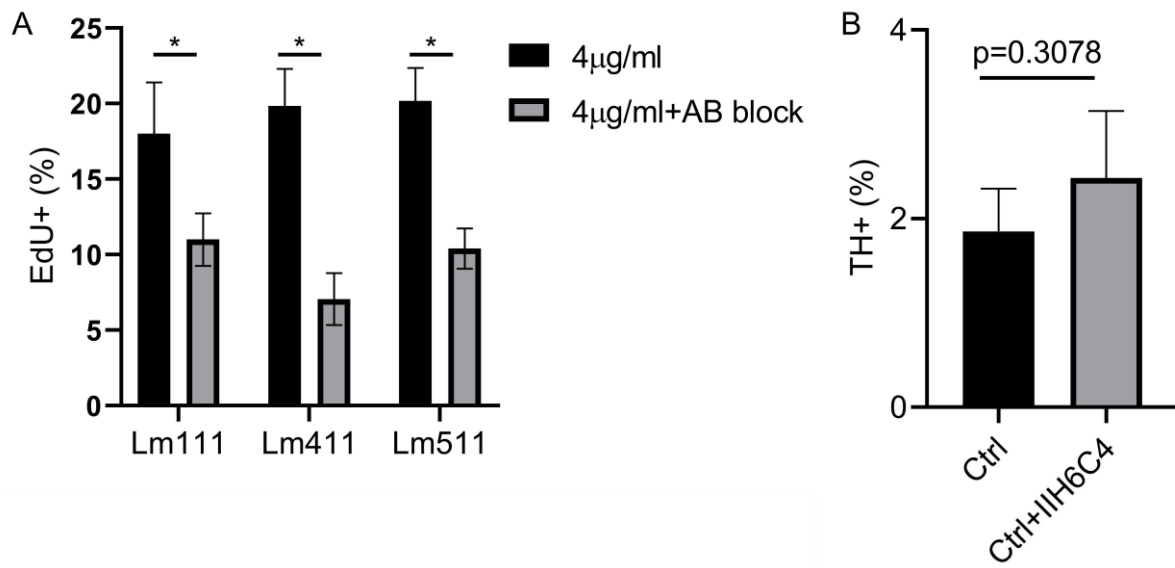


Fig S4: Expression of Im receptors

Integrins α6, α7, β1 and Dystroglycan are expressed in the mouse VM and on hES derived mDA progenitors at day 14 of culture. scRNA-seq of the hVM identifies radial glial (hRgl1-3) and VM progenitors (hProg) positive for Lm receptor expression. Right axis shows absolute molecule counts. Scale bar 50μm.

**Fig S5: Specificity of laminin-receptor interactions**

(A) Integrin $\alpha 6$ and $\alpha 7$ blocked with antibodies in the presence of 4 $\mu\text{g ml}^{-1}$ of Lm111, Lm411 and Lm511. When cultures are exposed to the integrin blocking antibodies, the Lm-driven increase in proliferation is abrogated suggesting that the integrin receptors are mediating the proliferative effects of Lm. (B) Blocking the α -dystroglycan receptor with no exogenous Lm211 does not effect the number of TH⁺ neurons generated. N=3, two-tailed unpaired t-test, *p<0.001.

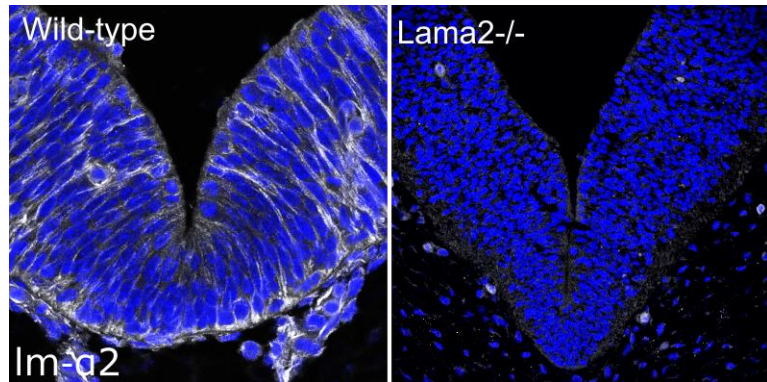
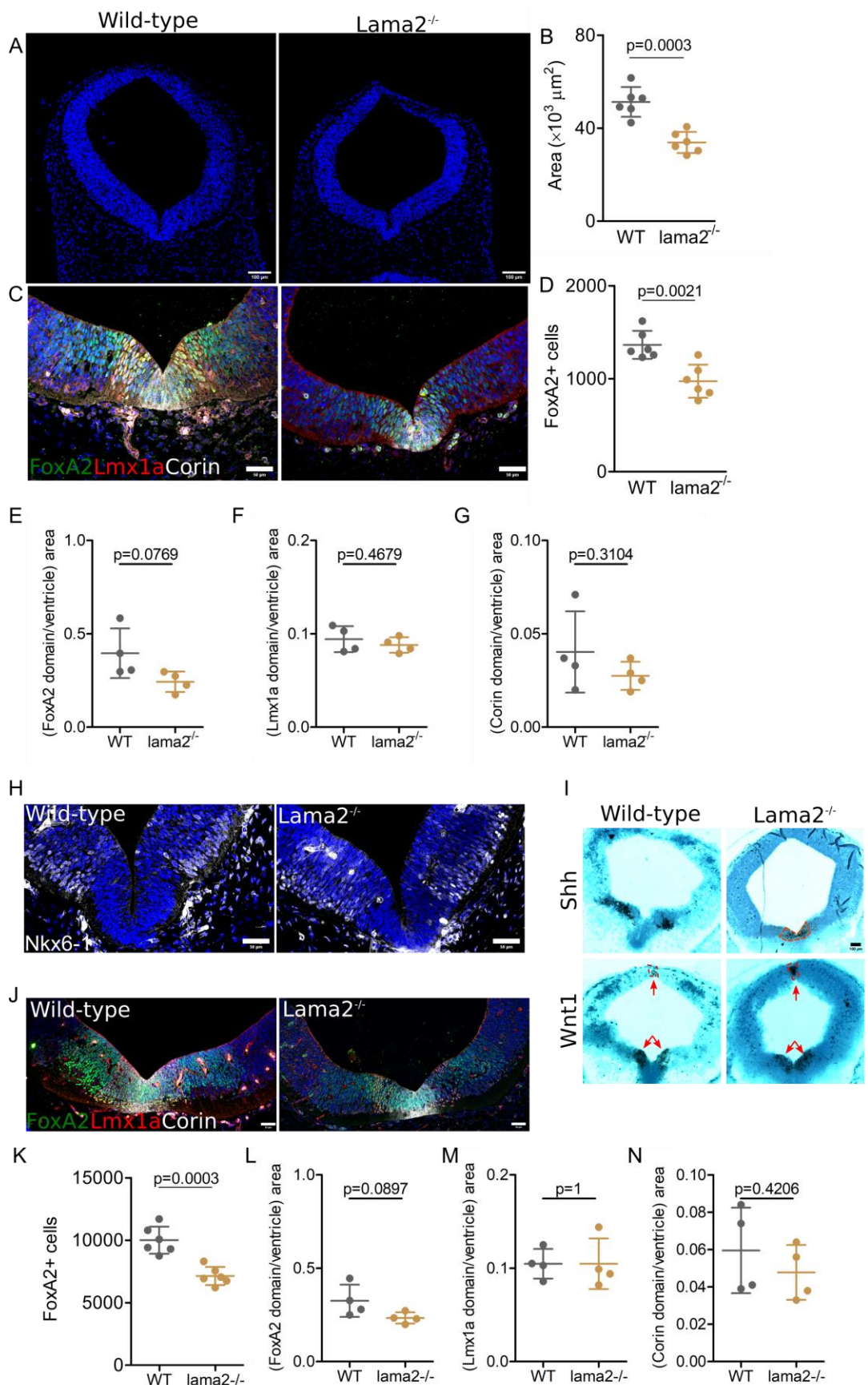


Fig S6: Lm- α 2 expression in the wild-type and *Lama2*^{-/-} mouse VM

No Lm- α 2 expression can be detected in the *Lama2*^{-/-} embryos confirming the knock-out.

**Fig S7: Lama2^{-/-} exhibit defects in growth but normal patterning**

(A) Cross-sections of wild-type and lama2^{-/-} mesencephalon at E10.5 (scale bar 100 μm) with the mutant mesencephalon significantly smaller in area (B). The dopaminergic domain consisting of

FoxA2, Lmx1a and Corin (scale bar 50 µm). Fewer FoxA2 cells are present in the *lama2^{-/-}* midbrain (D). The area of each domain was calculated and normalised to the area of the ventricle. No significant differences were detected in the size of the normalised FoxA2 (E), Lmx1a (F) and Corin (G). Nkx6-1+ cells can be seen laterally and are induced in both the mutant and wild-type embryo at E10.5 (scale bar 50 µm) (H). Potential ectopic expression and a delay in the lateral expansion and medial inhibition of Shh expression in the mutant embryos at E12.5 can be seen. Wnt1 expression is comparable to wild-type and previously published reports (scale bar 100 µm) (I). Dopaminergic domain remains smaller at E12.5 (scale bar 50 µm) (J) in the mutant embryo compared to wild-type, consisting of fewer FoxA2 cells (K) but when normalised for ventricle size, there are no significant differences in FoxA2 (L), Lmx1a (M) or Corin (N) domain size. N=4-6, two-tailed unpaired t-test.

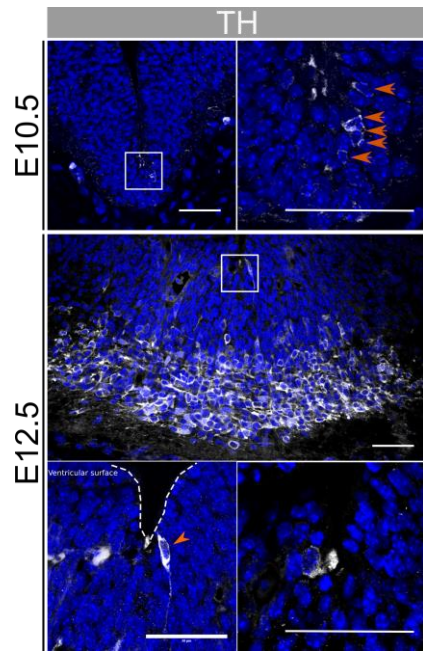


Fig S8: Ectopic mDA neurons in the VM of *lama2*^{-/-} embryos

TH+ mDA neurons can be seen lining the ventricular surface of *lma2* null embryos at E10.5 (orange arrows). Ectopic mDA neurons (orange arrowhead) at the ventricular surface (dashed line) continue to be observed at E12.5. Scale bar 50 μ m.

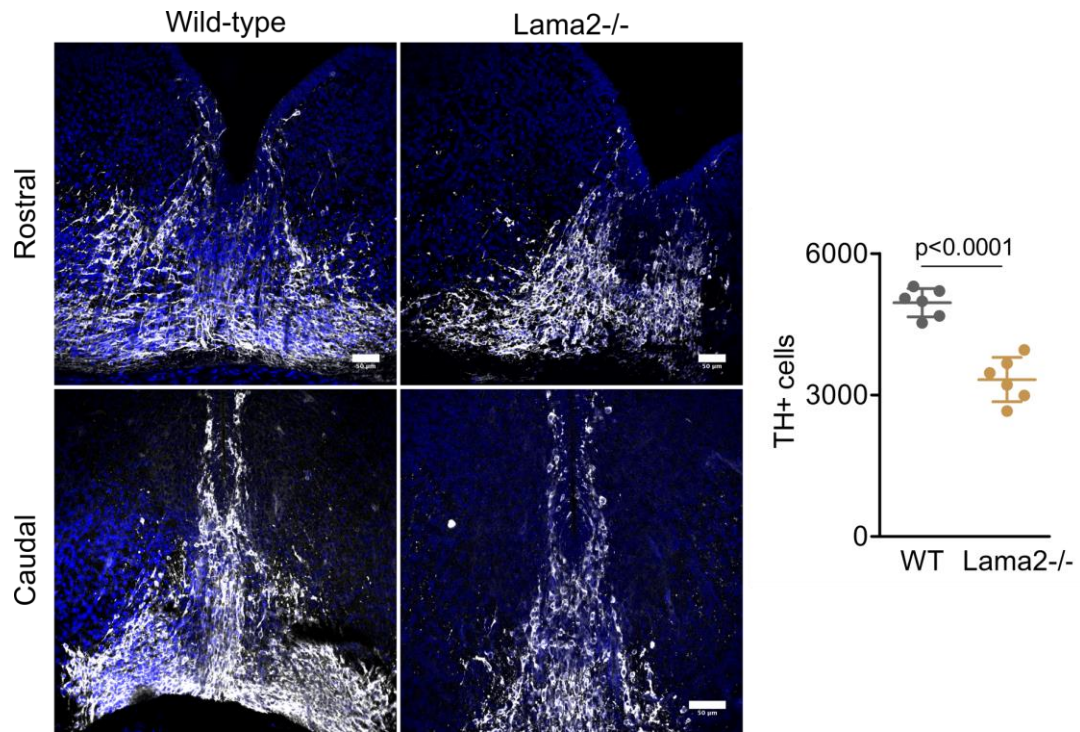


Fig S9: Reduced mDA neurons in the VM at E14.5

Significantly fewer TH⁺ mDA neurons in the VM of mutant embryos compared to wild-type littermate controls. N=6, two-tailed unpaired t-test, scale bar 50 µm.

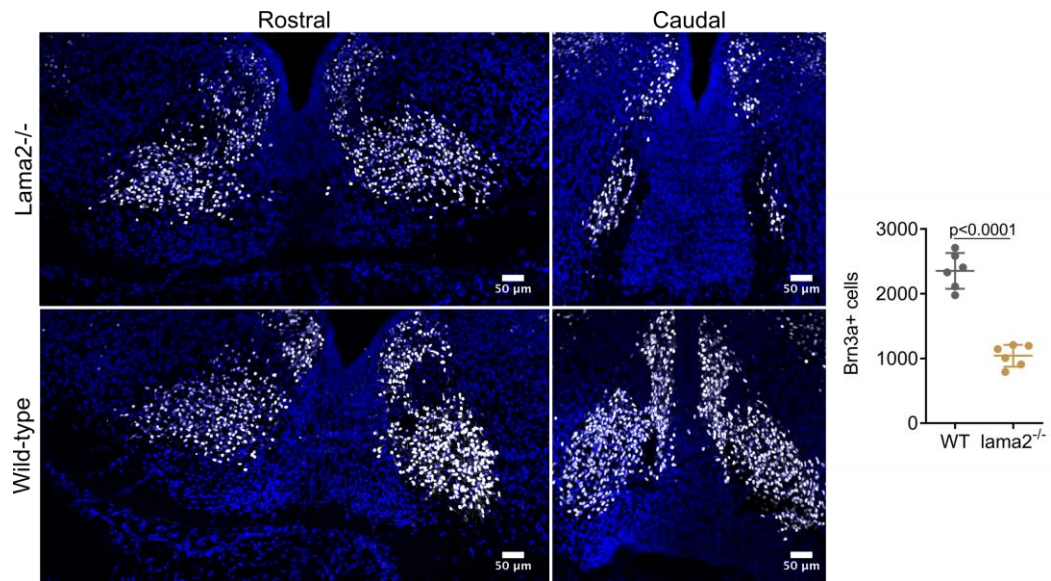


Fig S10: Development of non-mDA VM neurons compromised in *lama2*^{-/-} mutants.

Brn3a+ red nucleus neurons, derived from FoxA2+ progenitors, are significantly reduced in the mutant embryos compared to wild-type littermate controls at E14.5. N=6, two-tailed unpaired t-test, scale bar 50μm.

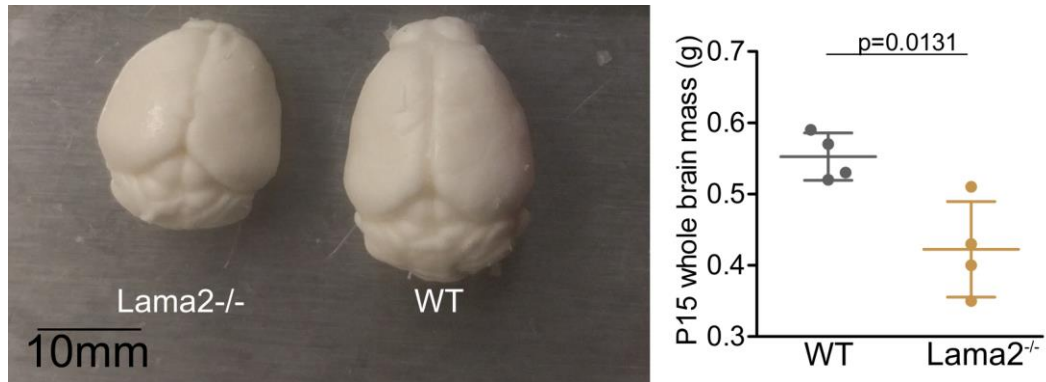


Fig S11: Smaller mutant brains compared to wild-types at P15

Lama2^{-/-} brains are significantly smaller than WT littermate controls, quantified via mass. N=4, two-tailed unpaired t-test.

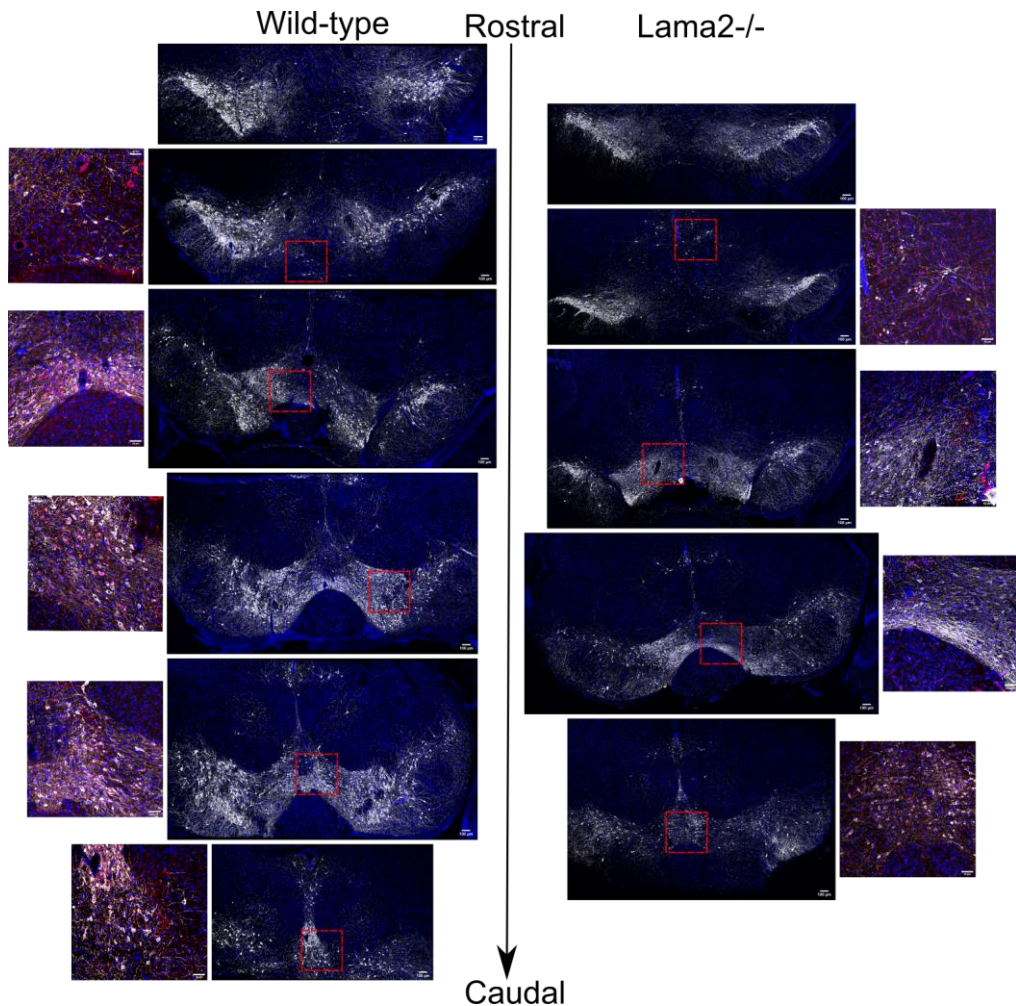


Fig S12: VM of wild-type and mutant P15 brains showing reduced number of neurons

Large panels are images of the whole VM from wild-type and *Lama2*^{-/-} P15 brains along the rostral-caudal axis showing reduced TH+ immunoreactivity (white) in the mutant brains (scale bar 100 µm). Images to the side are expanded view of the red boxes displaying TH (white) and Calb1 (red) (scale bar 50 µm). Fewer TH+ Calb1+ double positive cells can be seen in the mutant brains, particularly in the more caudal sections.

Table S1: List of Antibodies and dilutions used in this study. References detailing specificity of antibodies are provided.

Protein	Species	Company (cat.no.)	Dilution	Reference
Laminin α 1	Rabbit	Assay Biotech (C13064)	1:200	(Olsen et al., 1989)
Laminin α 2	Rabbit	Assay Biotech (C13065)	1:200	(Yap et al., 2019)
Laminin α 3	Rabbit	Assay Biotech (C13066)	1:200	(Ishihara et al., 2018)
Laminin α 4	Goat	R&D (AF3837)	1:400	(Yao et al., 2014)
Laminin α 5	Rabbit	Assay Biotech (C13068)	1:200	(Blanco et al., 2016)
Integrin α 6 [GoH3]	Rat	R&D (MAB13501)	1:500	(Sonnenberg et al., 1987)
Integrin α 7	Rabbit	Abcam (ab75224)	1:500	(Previtali et al., 2003)
Integrin β 1 [MB1.2]	Rat	Millipore (MAB1997)	1:500	(Von Ballestrem et al., 1996)
Dystroglycan [IIH6]	Mouse	SantaCruz (sc-53987)	1:1000	(Gee et al., 1994)
FoxA2 [M-20]	Goat	SantaCruz (sc-6554)	1:500	(Hatzis and Talianidis, 2002)
Ki67 [SP6]	Rabbit	Abcam (ab16667)	1:500	(Ekholm et al., 2014)
Nurr1 [N1404]	Mouse	Abcam (ab41917)	1:500	(Abasi et al., 2012)
TH	Rabbit	Millipore (AB152)	1:1000	(Ryczko et al., 2016)
Girk2	Goat	Abcam (ab65096)	1:500	(Fernandez-Alacid et al., 2011)
Calbindin	Mouse	Swant (300)	1:1000	(Martin del Campo et al., 2014)
Otx2	Goat	R&D (AF1979)	1:1000	(Sakai et al., 2017)
Oct4 [C-10]	Mouse	SantaCruz (sc-5279)	1:1000	(Kristensen et al., 2010)
Lmx1 α	Rabbit	Millipore (AB10533)	1:1000	(Laguna et al., 2015)
Nkx6.1	Mouse	DHSB (1:50)	1:100	(Pedersen et al., 2006)
aCaspase 3 [ASP175]	Rabbit	Cell Signalling (9661s)	1:500	(Wang et al., 2017)
Pax6	Rabbit	Abcam (ab5790)	1:200	(Tan et al., 2016)
Ngn2 [C-16]	Goat	SantaCruz (sc-19233)	1:1000	(Mazzoni et al., 2013)
Corin [231443]	Rat	Invitrogen (231443)	1:500	(Paik et al., 2018)
DDC	Goat	R&D (AF3564-SP)	1:250	(Sandmeier et al., 1994)
Pbx1a [710.2]	Mouse	SantaCruz (sc-101851)	1:250	(Villaescusa et al., 2016)

Reference:

- Abasi, M., Massumi, M., Riazi, G., Amini, H., 2012. The synergistic effect of beta-boswellic acid and Nurr1 overexpression on dopaminergic programming of antioxidant glutathione peroxidase-1-expressing murine embryonic stem cells. *Neuroscience* 222, 404–416. <https://doi.org/10.1016/j.neuroscience.2012.07.009>
- Blanco, S., Bandiera, R., Popis, M., Hussain, S., Lombard, P., Aleksic, J., Sajini, A., Tanna, H., Cortes-Garrido, R., Gkatza, N., Dietmann, S., Frye, M., 2016. Stem cell function and stress response are controlled by protein synthesis. *Nature* 534, 335–340. <https://doi.org/10.1038/nature18282>
- Ekholm, M., Beglerbegovic, S., Grabau, D., Lovgren, K., Malmstrom, P., Hartman, L., Ferno, M., 2014. Immunohistochemical assessment of Ki67 with antibodies SP6 and MIB1 in primary breast cancer: a comparison of prognostic value and reproducibility. *Histopathology* 65, 252–260. <https://doi.org/10.1111/his.12392>
- Fernandez-Alacid, L., Watanabe, M., Molnar, E., Wickman, K., Lujan, R., 2011. Developmental regulation of G protein-gated inwardly-rectifying K⁺ (GIRK/Kir3) channel subunits in the brain. *Eur. J. Neurosci.* 34, 1724–1736. <https://doi.org/10.1111/j.1460-9568.2011.07886.x>
- Gee, S.H., Montanaro, F., Lindenbaum, M.H., Carbonetto, S., 1994. Dystroglycan-alpha, a dystrophin-associated glycoprotein, is a functional agrin receptor. *Cell* 77, 675–686. [https://doi.org/10.1016/0092-8674\(94\)90052-3](https://doi.org/10.1016/0092-8674(94)90052-3)
- Hatzis, P., Talianidis, I., 2002. Dynamics of enhancer-promoter communication during differentiation-induced gene activation. *Mol. Cell* 10, 1467–1477.
- Ishihara, J., Ishihara, A., Fukunaga, K., Sasaki, K., White, M.J.V., Briquez, P.S., Hubbell, J.A., 2018. Laminin heparin-binding peptides bind to several growth factors and enhance diabetic wound healing. *Nat. Commun.* 9, 2163. <https://doi.org/10.1038/s41467-018-04525-w>
- Kristensen, D.M., Nielsen, J.E., Kalisz, M., Dalgaard, M.D., Audouze, K., Larsen, M.E., Jacobsen, G.K., Horn, T., Brunak, S., Skakkebaek, N.E., Leffers, H., 2010. OCT4 and downstream factors are expressed in human somatic urogenital epithelia and in culture of epididymal spheres. *Mol. Hum. Reprod.* 16, 835–845. <https://doi.org/10.1093/molehr/gaq008>
- Laguna, A., Schintu, N., Nobre, A., Alvarsson, A., Volakakis, N., Jacobsen, J.K., Gomez-Galan, M., Sopova, E., Joodmardi, E., Yoshitake, T., Deng, Q., Kehr, J., Ericson, J., Svenningsson, P., Shupliakov, O., Perlmann, T., 2015. Dopaminergic control of autophagic-lysosomal function implicates Lmx1b in Parkinson's disease. *Nat. Neurosci.* 18, 826–835. <https://doi.org/10.1038/nn.4004>
- Martin del Campo, H., Measor, K., Razak, K.A., 2014. Parvalbumin and calbindin expression in parallel thalamocortical pathways in a gleaning bat, *Antrozous pallidus*. *J. Comp. Neurol.* 522, 2431–2445. <https://doi.org/10.1002/cne.23541>
- Mazzoni, E.O., Mahony, S., Closser, M., Morrison, C.A., Nedelec, S., Williams, D.J., An, D., Gifford, D.K., Wichterle, H., 2013. Synergistic binding of transcription factors to cell-specific enhancers programs motor neuron identity. *Nat. Neurosci.* 16, 1219–1227. <https://doi.org/10.1038/nn.3467>
- Olsen, D., Nagayoshi, T., Fazio, M., Peltonen, J., Jaakkola, S., Sanborn, D., Sasaki, T., Kuivaniemi, H., Chu, M.L., Deutzmann, R., 1989. Human laminin: cloning and sequence analysis of cDNAs encoding A, B1 and B2 chains, and expression of the corresponding genes in human skin and cultured cells. *Lab. Investig. J. Tech. Methods Pathol.* 60, 772–782.
- Paik, E.J., O'Neil, A.L., Ng, S.-Y., Sun, C., Rubin, L.L., 2018. Using intracellular markers to identify a novel set of surface markers for live cell purification from a heterogeneous hIPSC culture. *Sci. Rep.* 8, 804. <https://doi.org/10.1038/s41598-018-19291-4>
- Pedersen, I.L., Klinck, R., Hecksher-Sorensen, J., Zahn, S., Madsen, O.D., Serup, P., Jorgensen, M.C., 2006. Generation and characterization of monoclonal antibodies

- against the transcription factor Nkx6.1. *J. Histochem. Cytochem. Off. J. Histochem. Soc.* 54, 567–574. <https://doi.org/10.1369/jhc.5A6827.2006>
- Previtali, S.C., Dina, G., Nodari, A., Fasolini, M., Wrabetz, L., Mayer, U., Feltri, M.L., Quattrini, A., 2003. Schwann cells synthesize alpha7beta1 integrin which is dispensable for peripheral nerve development and myelination. *Mol. Cell. Neurosci.* 23, 210–218.
- Ryczko, D., Cone, J.J., Alpert, M.H., Goetz, L., Auclair, F., Dube, C., Parent, M., Roitman, M.F., Alford, S., Dubuc, R., 2016. A descending dopamine pathway conserved from basal vertebrates to mammals. *Proc. Natl. Acad. Sci. U. S. A.* 113, E2440–2449. <https://doi.org/10.1073/pnas.1600684113>
- Sakai, A., Nakato, R., Ling, Y., Hou, X., Hara, N., Iijima, T., Yanagawa, Y., Kuwano, R., Okuda, S., Shirahige, K., Sugiyama, S., 2017. Genome-Wide Target Analyses of Otx2 Homeoprotein in Postnatal Cortex. *Front. Neurosci.* 11, 307. <https://doi.org/10.3389/fnins.2017.00307>
- Sandmeier, E., Hale, T.I., Christen, P., 1994. Multiple evolutionary origin of pyridoxal-5'-phosphate-dependent amino acid decarboxylases. *Eur. J. Biochem.* 221, 997–1002. <https://doi.org/10.1111/j.1432-1033.1994.tb18816.x>
- Sonnenberg, A., Janssen, H., Hogervorst, F., Calafat, J., Hilgers, J., 1987. A complex of platelet glycoproteins Ic and IIa identified by a rat monoclonal antibody. *J. Biol. Chem.* 262, 10376–10383.
- Tan, X., Liu, W.A., Zhang, X.-J., Shi, W., Ren, S.-Q., Li, Z., Brown, K.N., Shi, S.-H., 2016. Vascular Influence on Ventral Telencephalic Progenitors and Neocortical Interneuron Production. *Dev. Cell* 36, 624–638. <https://doi.org/10.1016/j.devcel.2016.02.023>
- Villaescusa, J.C., Li, B., Toledo, E.M., Rivetti di Val Cervo, P., Yang, S., Stott, S.R., Kaiser, K., Islam, S., Gyllborg, D., Laguna-Goya, R., Landreh, M., Lonnerberg, P., Falk, A., Bergman, T., Barker, R.A., Linnarsson, S., Selleri, L., Arenas, E., 2016. A PBX1 transcriptional network controls dopaminergic neuron development and is impaired in Parkinson's disease. *EMBO J.* 35, 1963–1978. <https://doi.org/10.15252/embj.201593725>
- Von Ballestrem, C.G., Uniyal, S., McCormick, J.I., Chau, T., Singh, B., Chan, B.M., 1996. VLA-beta 1 integrin subunit-specific monoclonal antibodies MB1.1 and MB1.2: binding to epitopes not dependent on thymocyte development or regulated by phorbol ester and divalent cations. *Hybridoma* 15, 125–132. <https://doi.org/10.1089/hyb.1996.15.125>
- Wang, Y., Gao, W., Shi, X., Ding, J., Liu, W., He, H., Wang, K., Shao, F., 2017. Chemotherapy drugs induce pyroptosis through caspase-3 cleavage of a gasdermin. *Nature* 547, 99–103. <https://doi.org/10.1038/nature22393>
- Yao, Y., Chen, Z.-L., Norris, E.H., Strickland, S., 2014. Astrocytic laminin regulates pericyte differentiation and maintains blood brain barrier integrity. *Nat. Commun.* 5, 3413. <https://doi.org/10.1038/ncomms4413>
- Yap, L., Wang, J.-W., Moreno-Moral, A., Chong, L.Y., Sun, Y., Harmston, N., Wang, X., Chong, S.Y., Ohman, M.K., Wei, H., Bunte, R., Gosh, S., Cook, S., Hovatta, O., de Kleijn, D.P.V., Petretto, E., Tryggvason, K., 2019. In Vivo Generation of Post-infarct Human Cardiac Muscle by Laminin-Promoted Cardiovascular Progenitors. *Cell Rep.* 26, 3231–3245.e9. <https://doi.org/10.1016/j.celrep.2019.02.083>